Journal of Membrane Science 499 (2016) 156–163

Contents lists available at ScienceDirect

Journal of Membrane Science

journal homepage: www.elsevier.com/locate/memsci

Proton conducting poly(vinyl alcohol) (PVA)/ poly (2-acrylamido-2-methylpropane sulfonic acid) (PAMPS)/ zeolitic imidazolate framework (ZIF) ternary composite membrane

Mustafa Erkartal [a], Hakan Usta [a], Murat Citir [a], Unal Sen [b,*]

[a] Abdullah Gül University, Department of Materials Science and Nanotechnology, 38080 Kayseri, Turkey
[b] Abdullah Gül University, Department of Mechanical Engineering, 38080 Kayseri, Turkey

ARTICLE INFO

Article history:
Received 19 August 2015
Received in revised form
10 October 2015
Accepted 12 October 2015
Available online 23 October 2015

Keywords:
PVA
PAMPS
ZIF-8
Proton exchange membrane

ABSTRACT

The design, synthesis and characterization of novel proton exchange membranes (PEMs) are of significant scientific and technological importance for the realization of fuel cells, actuators, and sensors. Here, we demonstrate a novel ternary composite membrane consisting of poly(vinyl alcohol) (PVA), poly (2-acrylamido-2-methylpropane sulfonic acid) (PAMPS), zeolitic imidazolate framework-8 (ZIF-8), which is prepared by physical blending and casting methods. To enhance the water management of the membranes, in situ chemical cross-linking is carried out by glutaraldehyde (GA). During the characterization of the new membranes, FT-IR is used for intermolecular and inter-polymer interactions between different components of the membrane, SEM is used to identify morphology, XRD is used to prove the presence of ZIF-8 nanoparticles, and finally TGA is used for thermal stability. The proton conductivity of the membranes is found to increase with temperature and also with the increasing content of PAMPS. The highest proton conductivity under fully hydrated state at 80 °C is measured as 0.134 S cm^{-1} for PVA: PAMPS: ZIF-8 (55:40:5) composition. In this study, it is clearly shown that ZIF-8 nanoparticles contribute to the proton conductivity by forming hydrogen bonds with the polymer network in the membrane. The water uptake (WU) and ion exchange capacity (IEC) values are 3.28 (g/g) and 1.52 meq g^{-1}, respectively for the same membrane. To the best our knowledge, this study shows one of the first example of a MOF-containing membrane with truly high proton conductivities, and both values of proton conductivity and electrochemical properties are comparable to those of well-studied membrane, Nafion.

1. Introduction

Proton exchange membrane fuel cell (PEMFC) technology is an innovative research area, which has attracted significant attention over the past few decades for the realization of next-generation power sources. Owing to their extremely low greenhouse gas emissions, high energy conversion efficiencies, fuel variety, and low maintenance costs, PEMFCs are expected to emerge in various energy-driven applications including portable, stationary and transportation sectors [1]. In a typical PEMFC, the main part of the device is an electrolyte membrane, which is responsible to provide H^+ ions for the proton conductivity process from cathode to anode. Good proton conductivity is the most important feature expected from a PEM. In addition to high proton conductivity, a desirable membrane should be impermeable to fuel molecules such as H_2 and CH_3OH, in order not to allow crossover between anode and cathode. Finally, they should exhibit good thermal, chemical and mechanical stabilities under device operation condition.

Today, the most common membranes are based on perfluorosulfonic acid structures; Nafion is the most well-known example as a trademark of Dupont. In Nafion, while the PTFE backbone provides mechanical and dimensional stability, ionically bonded sulfonic acid functional groups enable proton transfer across the membrane. Despite these advantageous properties, it has several drawbacks such as high cost, methanol crossover and rapid decrease of proton conductivity above 80 °C [2–6]. On the other hand, physically blended membranes consisting of a hydrocarbon matrix has significantly drawn attention because they are cost-effective, highly impermeable to methanol, and they show high water selectivity [3,4,7–9]. Polyvinylalcohol (PVA) has been widely used as a matrix in blended membranes because of its facile film-forming film ability, hydrophilic nature, and chemical/ mechanical stability [10–13]. PVA has a high tendency to attract water and it can be even dissolved in water at room temperature. However, thanks to the presence of –OH functional groups, PVA

* Corresponding author.
E-mail address: unal.sen@agu.edu.tr (U. Sen).

http://dx.doi.org/10.1016/j.memsci.2015.10.032
0376-7388/

can be effectively cross-linked by bis(aldehydes), resulting in remarkable improvements in their thermal and mechanical stabilities. Another drawback of PVA that restrains its single component utilization as a fuel cell membrane is its poor proton conductivity [8,13].

Poly(2-acrylamido-2-methyl-1-propanesulfonic acid) (PAMPS) is an acidic polymer that constitutes from acidic monomers of AMPS (2-acrylamido-2-methylpropanesulfonic acid), and it typically shows higher proton conductivity compared to partially hydrated Nafion [14,15]. As a result of its unique chemical structure, PAMPS exhibits high water uptake affinity with much better dimensional stability in comparison to Nafion and polystyrenesulfonicacid (PSSA). Therefore, it is an ideal membrane material for fuel cell applications at high temperatures. However, since PAMPS homopolymer suffers from water, it could not be used as its pristine form in a membrane [16].

Metal organic frameworks (MOFs) are a new class of ordered porous materials. They consist of inorganic metal clusters and organic linkers. Since the chemical structures of the metal centers and the linkers can be designed by synthetic tailoring to obtain the desired properties for a certain application, MOFs have recently attracted significant scientific and technological attention from diverse research disciplines [17–19]. In addition to gas adsorption and separation, catalysis, sensing and gas storage, recently there is a growing interest on the proton conducting properties of such materials. From a material design perspective, high porosity of MOFs enables the formation of pathways through which protons can be carried properly [20]. Several studies have revealed that many MOFs possess considerable proton conductivity below 100 °C under high humidification [19,21–25].

In this study, we envision that a new ternary composite proton exchange membrane embedding poly(vinyl alcohol), poly(2-acrylamido-2-methylpropane sulfonic acid) (PAMPS), and zeolitic imidazolate framework-8 (ZIF-8) may exhibit high proton conductivity and good chemical and mechanical properties. In this novel design, PVA is used as the main matrix material due to its favorable film-forming ability and mechanical properties. To enhance its swelling properties, cross-linking was performed by using glutaraldehyde, which creates an $-O(CH_2)_5O-$ linker between hydroxyl groups (–OH) of PVA [13]. PAMPS does not only serve as the primary proton donor in the membrane system but also acts as a catalyst for the acetalization cross-linking reaction instead of HCl [8]. Zeolitic imidazolate frameworks (ZIFs) are a sub-class of MOFs which have similar pore topologies with zeolites, and show superior chemical and thermal stabilities. The MOF used in this design, ZIF-8, consists of Zn (II) metal cation centers linked with 2-methylimidazolate (Hmim) anion in the tetrahedral framework that forms the sodalite (SOD) zeolite structure with large cavities (11.6 Å) and small pore size (3.4 Å) [26–28]. As a result of Hmim linkers, ZIF-8 is highly hydrophobic [29–31] that provides a high water stability for the framework when it's in contact with water. In consequence of its hydrophobic nature and better compatibility with polymer matrix, ZIF-8 is expected to improve water management of the new membrane, while assisting the proton conduction.

2. Experimental

2.1. Materials

2-Methylimidazole (Hmim with 97% purity) and Zinc Nitrate Hexahydrate (Zn $(NO_3)_2.6H_2O$, 99% purity – metal based) were purchased from Alfa Aesar. PAMPS (Mw=2,000,000, 15 wt% in aqueous), PVA (M_w=89,000–98,000, more than 99% hydrolyzed) and Gluturaldeyde solution (GA, 25 wt% aqueous) were purchased from Sigma-Aldrich. Methanol with 99.9% purity was purchased from Merck.

2.2. Synthesis of ZIF-8 nanoparticles

In the synthesis of the ZIF-8 nanoparticles, a reported procedure was followed [32]. A solution of 1.0510 g (3.53 mmol) $Zn(NO_3)_2 \cdot 6H_2O$ in 50 ml of methanol was poured into a solution of 2.3353 g (28.3 mmol) Hmim in 50 ml of methanol. Then, the resulting solution was vigorously stirred at room temperature for 1 h. At the end of the stirring process, the milky solution was centrifuged at 7500 rpm two times to obtain the desired nanoparticles, which were washed by methanol. Finally, some part was heated in a vacuum oven at 80 °C for 24 h for further characterization, and the rest of the nanoparticles were kept in methanol for the next steps. The yield of ZIF-8 synthesis was ~30% based on Zn.

2.3. Membrane preparation

The PVA/PAMPS/ZIF-8-based matrix membrane was prepared by solution casting method. First, a desired amount of powder PVA was fully dissolved in distilled water at 80 °C by stirring to yield a 10 wt% solution. Next, a certain amount of ZIF-8 in methanol was poured into PVA solution at room temperature. The suspension was then vigorously stirred for 12 h. Afterwards, appropriate amount of PAMPS in water was slowly added to the prepared solution, and the resulting solution was stirred vigorously for 12 h at room temperature. The cross-linking was carried out in situ by adding 0.1 ml GA (25 wt% in water). It's noteworthy that no additional acidic catalyst is needed for the cross-linking reaction since PAMPS provides in situ protons for this reaction. As the final step, the blend was cast onto a glass petri dish. In order to remove residual solvents from the cast films, they were first placed in a chemical hood under ventilation overnight, which is followed by further vacuum drying (~100 mTorr) in an oven at 70 °C for 4 h. The final concentrations of PAMPS in all films were 10, 20, 30, and 40 wt% (Fig. 1).

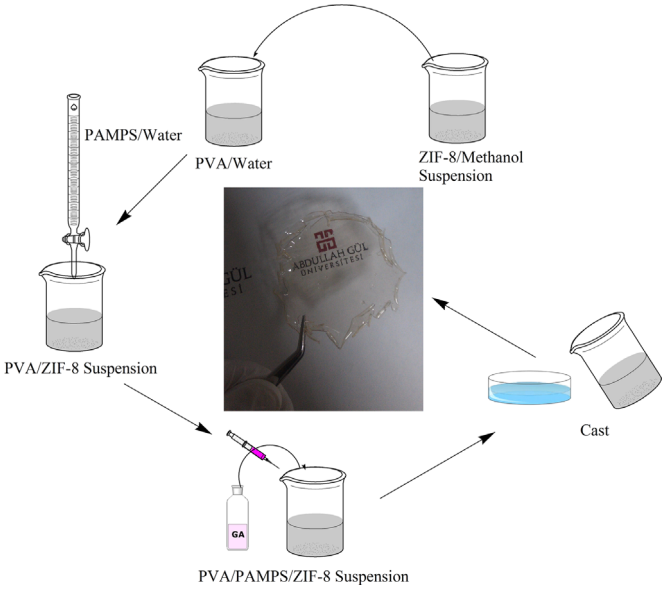

Fig. 1. The scheme for the preparation of the ternary composite membranes.

2.4. Characterization

2.4.1. X-ray diffraction (XRD)

X-ray diffraction pattern of the prepared membranes were acquired by using Bruker AXS D8 Advance. The diffraction angle (2θ) range from 5° to 40° was scanned at a scan rate 0.010 min^{-1} with 1.54 nm wavelength radiation, which is generated by CuKα.

2.4.2. Fourier Transform Infrared Spectroscopy (FT-IR)

The prepared membrane was examined by using Attenuated Total Reflectance Fourier Transform Spectroscopy (ATR-FTIR) on Thermo Nicolet 6700. Spectrum was obtained with 4 cm^{-1} resolution between 400–4000 cm^{-1}.

2.4.3. Scanning Electron Microscopy (SEM)

The morphologies of the prepared membranes were examined by Zeiss EVO LS 10. To affirm the existence and homogenous distributions of the ZIF-8 nanoparticles in the composite membrane, elemental mapping was carried out via energy-dispersive X-ray spectroscopy.

2.4.4. Proton conductivity

Proton conductivity measurements of the prepared membranes were performed using a Novocontrol dielectric-impedance analyzer. The films were sandwiched between platinum blocking electrodes, and the conductivity was measured in the frequency range from 1 Hz to 3 MHz as a function of temperature (20, 40, 60, and 80 °C).

2.4.5. Thermogravimetric Analysis (TGA)

Thermal degradation of the membranes and ZIF-8 nanoparticles was examined by Shimadzu DTG 60. Before the measurements, all membranes were held at 65 °C under vacuum for 12 h. All thermal measurements were carried out under nitrogen at a heating rate of 10 °C min^{-1}.

2.4.6. Water Uptake

The water uptake (WU) studies of the prepared membranes were performed in accordance with a reported procedure [33]: square pieces of the membrane samples with known dimensions (1×1 cm^2 square pieces) were dried at 65 °C to evaporate residual solvent, and then weighed. Next, dry membranes were soaked in deionised water for 24 h, surface water was properly wiped by a filter paper and weighed. Water uptake of the membranes was calculated using the following equation:

$$WU = \frac{(W_{wet} - W_{dry})}{W_{dry}} \quad (1)$$

where W_{wet} and W_{dry} are the wet and dry mass of the membranes. The WU experiments were repeated three times to ensure the accuracy.

2.4.7. Ion-exchange capacity

The ion exchange capacity (IEC) values of the prepared membranes were determined by titration following a reported procedure [33]. Firstly, the sample pieces were cut from the membrane and dried at 65 °C under vacuum. Then, membranes were immersed in 25 mL of 2 M NaCl aqueous solution to replace the H^+ by Na^+. Afterward, the solution was titrated with 0.1 M NaOH solution using a phenolphthalein indicator. The IEC is expressed in terms of milliequivalents of sulfonic groups per gram of dried sample. The IEC experiments were repeated three times to ensure the accuracy.

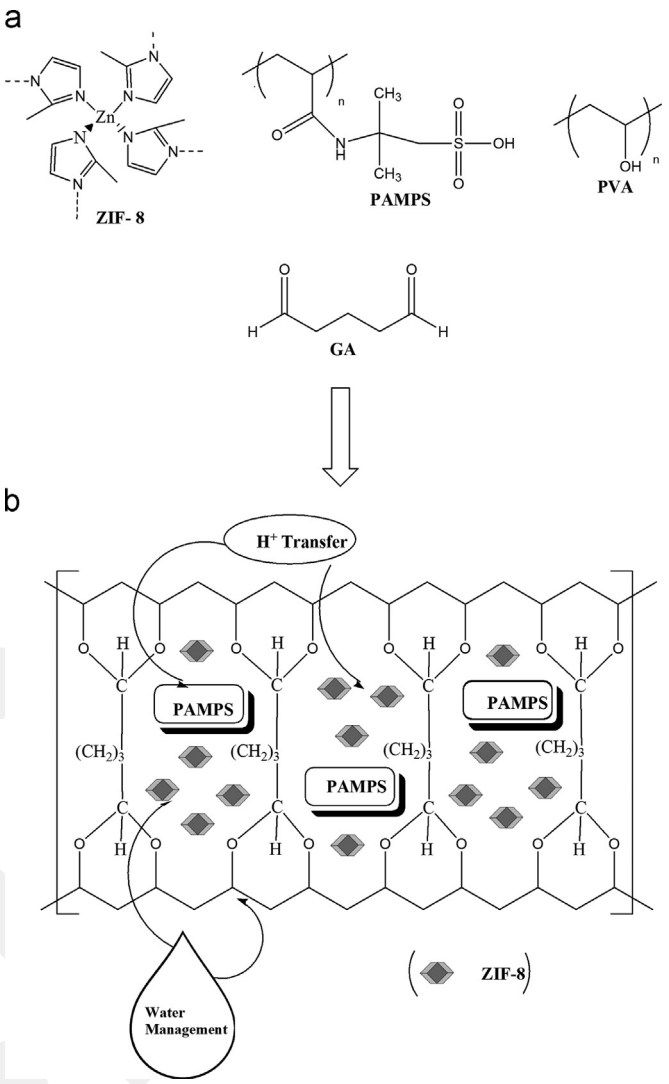

Fig. 2. (a) The chemical structures of ZIF-8, PAMPS, PVA, and GA. (b) Proposed chemical structure for the cross-linked PVA/PAMPS/ZIF-8 composite membrane.

3. Results and discussion

3.1. Structure of the PVA/PAMPS/ZIF-8 membrane

The proposed membrane structure is shown in Fig. 2b. All prepared membranes, regardless of their composition, are flexible, transparent and colourless. (Fig. 1) The thicknesses are 120–150 μm. In the design, PVA constitutes the framework of the membrane structure as the host polymer, and the chemical cross-linking reactions take place between hydroxyl groups (–OH) of PVA and aldehyde groups (–CHO) of GA to form cyclic acetals. In this way, swelling behaviour of the membrane is controlled and the membrane gains strength against water permeation. The trapped PAMPS chains in the PVA network participate in proton conductivity via its sulfonic acid groups (–SO_3H). ZIF-8 nanoparticles (40–60 nm) are dispersed homogenously through the membrane. These nanoparticles do not only assist the water management because of their hydrophobic nature, but also contribute to the proton conductivity by forming hydrogen bonds with the polymer network.

3.2. X-ray diffraction (XRD)

XRD patterns of synthesized ZIF-8 and membranes with

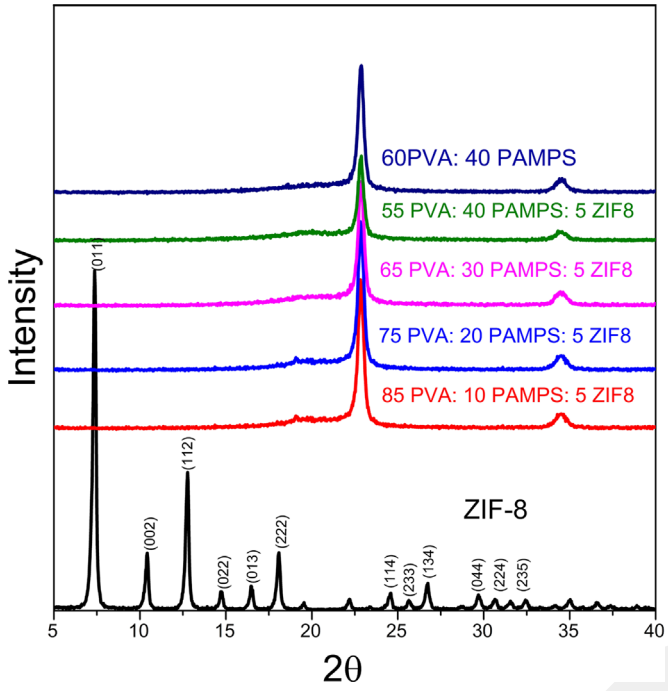

Fig. 3. XRD pattern of ZIF-8 and the ternary composite membranes with different compositions.

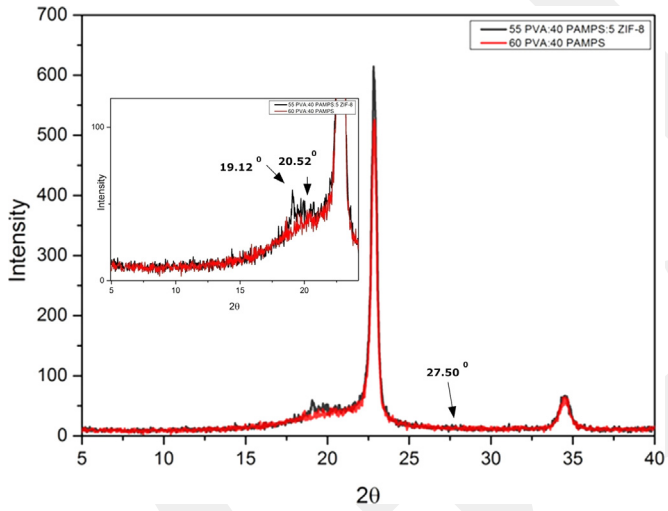

Fig. 4. Comparison of XRD pattern of the membrane with and without ZIF-8.

different PAMPS loadings are shown in Fig. 3. The diffraction peaks obtained for the ZIF-8 nanoparticles are in-line with the XRD pattern reported in the literature [25,26,32]. Cross-linked blended membranes shows two observable peaks at 2θ values of 22.8° and 35°. The sharp peak located at 2θ=22.8° corresponds to (101) plane of the semi-crystallized PVA [34,35]. As observed Fig. 3, there are no agglomerations in the blended membranes which contain ZIF-8, since the ratio of ZIF-8 in mass is very low and ZIF-8 nanoparticles are well distributed in the membrane because of their partially organic nature. On the other hand, Fig. 3 shows the existence of ZIF-8 nanoparticles in the membrane. In comparison with the pattern of PVA: PAMPS (60:40) membrane, there are some weak peaks appearing at 2θ values of 19.12°, 20.52° and 27.50° in the pattern of PVA:PAMPS:ZIF-8 (55:40:5) membrane. This is illustrated in Fig. 4. In addition, the membrane consisting of only ZIF-8 has relatively higher intensity peak at 2θ=22.8° compared that of the membrane consisting of only PVA and PAMPS.

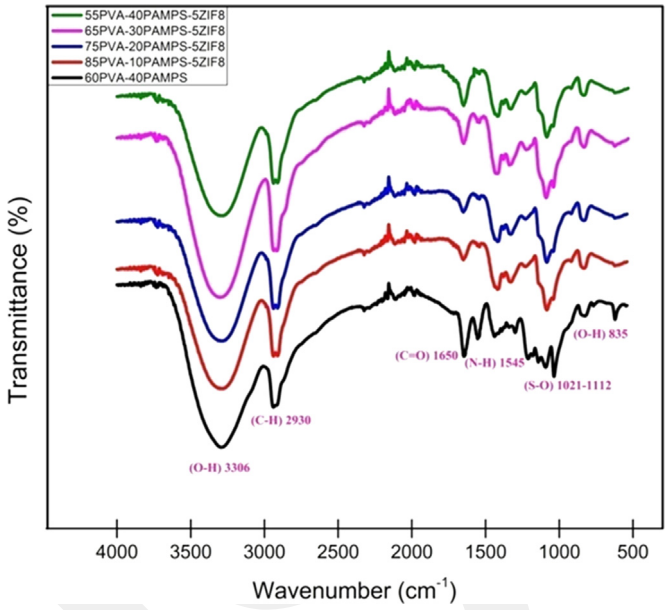

Fig. 5. FT-IR spectra of the composite membranes with different compositions.

These results clearly indicate that ZIF-8 nanoparticles in the membrane act as nucleation sites resulting in improved membrane crystallinity [35]. PAMPS is found to be in an amorphous state with almost no crystalline phase [14,16].

3.3. Fourier Transform Infrared Spectroscopy (FT-IR)

ATR/FT-IR was used in order to determine intra-/intermolecular interactions and hydrogen bonding between host polymers and ZIF-8 nanoparticles, and to identify the existence of crosslinking reactions between PVA and GA. Transmittance FT-IR spectra of the PVA/PAMPS/ZIF-8 ternary membranes and PVA/PAMPS binary membrane are shown in Fig. 5. The absorption peaks occurred in all spectra around at 3306 cm^{-1} and 2930 cm^{-1} are associated with (O–H) stretching and asymmetrical stretching of methylene (C–H) group in PVA chains, respectively [2–4,36]. The sharp peaks at about 1650 cm^{-1} and 1545 cm^{-1} are assigned to vibration of (C=O) and (N–H) group in PAMPS [2,8,37,38]. While the intensity of the signal coming from the (C=O) group increases with increasing the content of PAMPS in all membranes, the intensity of the vibrational peak of (N–H) groups decreases with inreasing amount of PAMPS for ZIF-8 containing ternary membranes. The plausible explanation to this result is the occurrence of intermolecular hydrogen bonding between non-defect-free ZIF-8 nanoparticles and (N–H) groups in the PAMPS polymeric chains. As shown in Fig. 5, the sharp peaks located at around 1021 and 1112 cm^{-1} correspond to (S–O) stretching of sulfonic acid groups in PAMPS [2,8,37–39]. In addition, the weak signal at 835 cm^{-1} is attributed to the bending of (O–H) due to free (–CHO) group coming from excess GA [8]. However, the characteristic peaks of the ZIF-8 could not be seen in this spectra. The reasons are that relatively small amount of ZIF-8 is present in the membranes, and the characteristic peaks of ZIF-8 overlaps with those of the polymer host. For instance, in the region of 3125–2929 cm^{-1}, aromatic (C–H) stretch of imidazoles [32] in ZIF-8 overlaps with the broad (O–H) stretches of PVA, and the (N=C) stretching of ZIF-8 coincides with the vibrations of amide groups in PAMPS. On the other hand, the formation of hydrogen bond between hydroxyl groups of PVA and sulfonic acid groups in PAMPS could not be determined independently due to the overlapping of hydrogen bonding between $-SO_3H\cdots HO-$ and $-OH\cdots HO-$ [37].

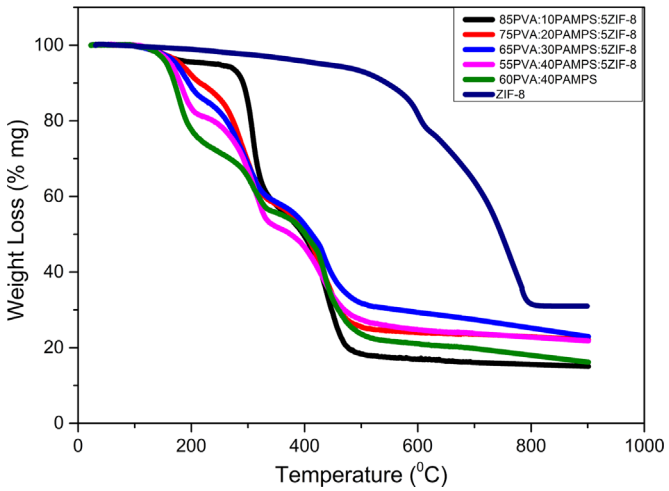

Fig. 6. Thermogravimetric analysis (TGA) thermograms of ZIF-8 and the composite membranes with different compositions.

3.4. Thermo-gravimetric analysis (TGA)

Fig. 6 shows the thermal degradation termograms of the membranes containing PVA-PAMPS-ZIF-8 membranes with different PAMPS and PVA contents and also pure ZIF-8. The membrane samples were dried under vacuum at 80 °C and kept under vacuum until the measurement. As shown in Fig. 6, three major stages of the thermal decomposition can be considered. The first stage of the decomposition, which occurs between 150 and 230 °C, is the degradation of the sulfonic acid groups (–SO_3H) in PAMPS. The second decomposition stage begins at around 230 °C and finishes at about 350 °C, which is attributed to cleavage of the side-chain of PVA. The final major decomposition step comes about between 330 and 540 °C, which is ascribed to cleavage of the backbone of the PVA [2,3,35,37,38]. As presented in Fig. 6, a long plateau is observed up to 500 °C, which indicates high thermal stability of ZIF-8 nanoparticles. A gradual weight loss of about 8 wt% is attributed to the removal of residual solvents and/or reactant molecules trapped in the nanocrystals during synthesis [32,35].

In this work and related earlier studies, it was observed that the pure PVA polymer remains stable up to 300 °C. However, with the addition of PAMPS, blend membranes exhibited a lower thermal stability, and higher PAMPS content leads to an early decomposition onset, and the weight loss becomes gradual. The differences in PAMPS content and the existence of ZIF-8 nanoparticles in the membranes result in significant differences in total weight drops of the blend membranes. For instance, the remained mass for the composition of PVA:PAMPS:ZIF-8 (85:10:5) was much lower than that of the PVA:PAMPS:ZIF-8 (55:40:5). Moreover, the total weight drops for all compositions of ZIF-8 containing membranes, except the one consisting of 10 wt% PAMPS membrane, are considerably lower than that of PVA:PAMPS (60:40). These results clearly indicate that there is a significant interaction between PAMPS and ZIF-8.

3.5. Scanning Electron Microscopy (SEM) and Energy Dispersive X-Ray Spectroscopy (EDX)

Fig. 7 presents the SEM images of the synthesized ZIF-8 nanoparticles. As it can be seen from Fig. 7, the size of the nanoparticles varies from 40 nm to 60 nm.

Cross sectional SEM micrographs of the blended membranes for different PAMPS loadings are given in Fig. 8. Apparently, the existence of small amounts of ZIF-8 nanoparticles in the membrane did not cause any considerable difference on the morphology of the membranes. Thus, we can conclude that ZIF-8 nanoparticles are homogenously distributed through the membrane network. The cross-sectional micrographs prove that there are no voids or agglomerations at the inter-phase regions.

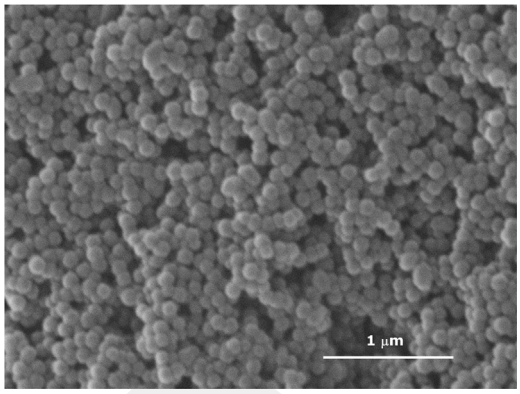

Fig. 7. SEM micrographs of ZIF-8 nanoparticles with higher magnification (100 k ×).

EDX mapping micrographs further confirm the homogenous distribution of ZIF-8 nanoparticles through the membrane. In this technique, the mapping of Zn and S elements is performed by using the energy dispersive X-ray spectroscopy to better understand the distribution of ZIF-8 and PAMPS, respectively, in the membrane. As shown in Fig. 9, EDX mapping micrographs indicate uniform distribution of Zn elements, and thus uniform distribution of ZIF-8 nanoparticles in the composite membrane. Additionally, these results indicate that the distribution of the PAMPS in the membrane is also homogenous.

3.6. Water uptake (WU) and ion exchange capacity (IEC)

The water uptake (WU), in other words swelling behavior, has a significant function for both migration of the protons along the membrane and the dimensional stability of the membrane under the operation conditions. In general, high water uptake values for the membranes lead to high proton conductivities. However, the excessive water uptake values in the membranes can cause some weakness on dimensions of the membranes and their thermal properties [2,4,33,37,40,41]. The water uptake values of the membranes are shown in Table 1. The hydrophilic parts of the membranes mainly determine water uptake performance. Obviously, PVA has a large tendency towards water due to its hydrophilic (–OH) functional groups, but in our design the polymer gains flexibility and mechanical strength via chemical cross-linking [8,13]. On the other hand, because of the imidazole linkers, ZIF-8 shows natural hydrophobic characteristics [29–31]. Hence, the water uptake values of the membrane is mainly governed by the PAMPS content in the membrane. It is well known that sulfonic acid groups (–SO_3H) are highly hydrophilic [16]. Therefore, as shown in Table 1, the WU values increase with increasing the content of PAMPS in the membranes. The measured water uptake values increase from 2.13 to 3.28. However, in comparison with PVA:PAMPS (60:40), the membrane with PVA:PAMPS:ZIF-8 (55:40:5) composition has slightly higher water uptake. The reason is that adsorbed water in ZIF-8 pores increases the water uptake values of the membrane despite the hydrophobic nature of ZIF-8.

The number of exchangeable ion groups in the membrane is determined by ion exchange capacity (IEC) of the membrane. Generally, IEC is given in terms of the moles of fixed SO_3^{-1} sites per gram of polymer. IEC affects the proton conductivity

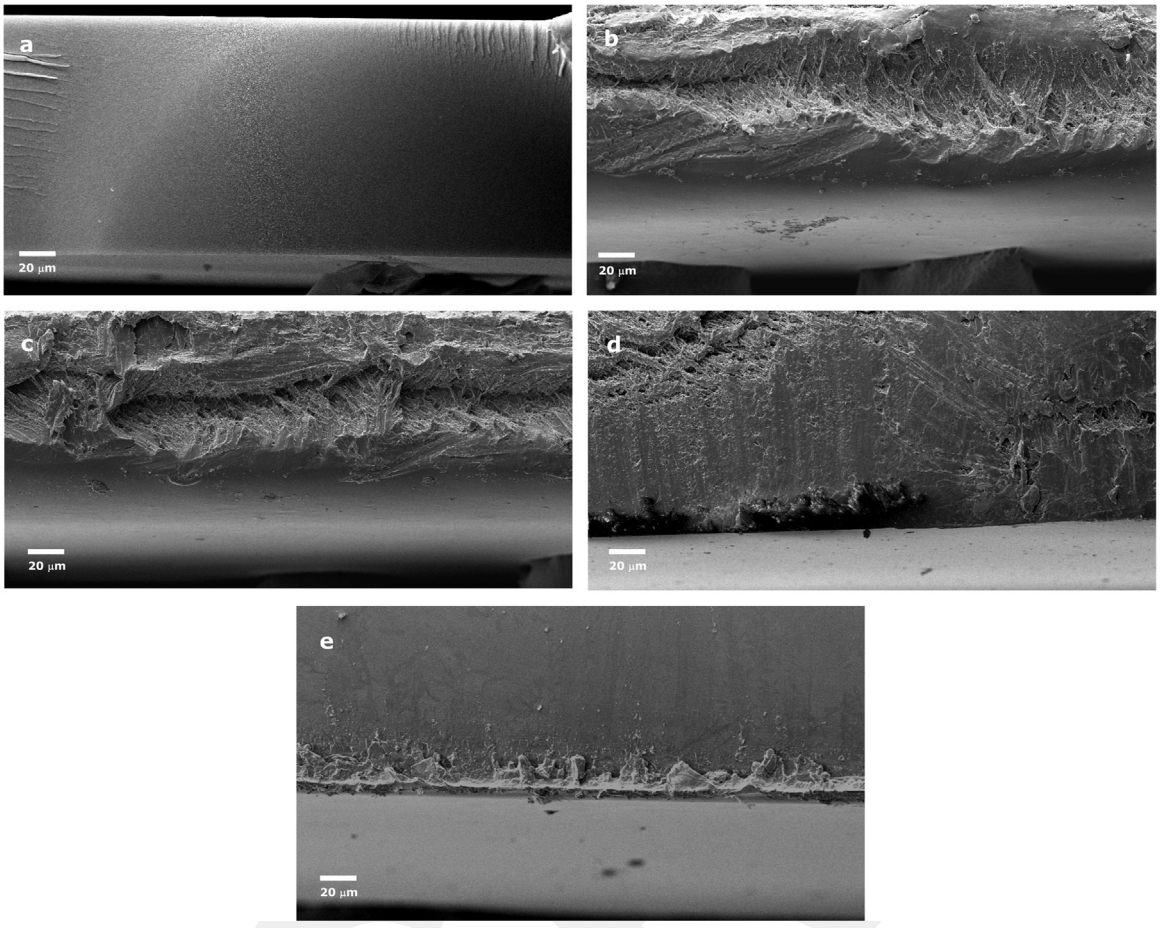

Fig. 8. Cross-sectional SEM micrographs of the membranes with different PAMPS loading (magnification of 2500 ×): (a) PVA:PAMPS (60:40), (b) PVA: PAMPS: ZIF-8 (85:10:5) (c) PVA: PAMPS: ZIF-8, (75:20:5) (d) PVA: PAMPS: ZIF-8 (65:30:5), and (e) PVA: PAMPS: ZIF-8 (55:40:5).

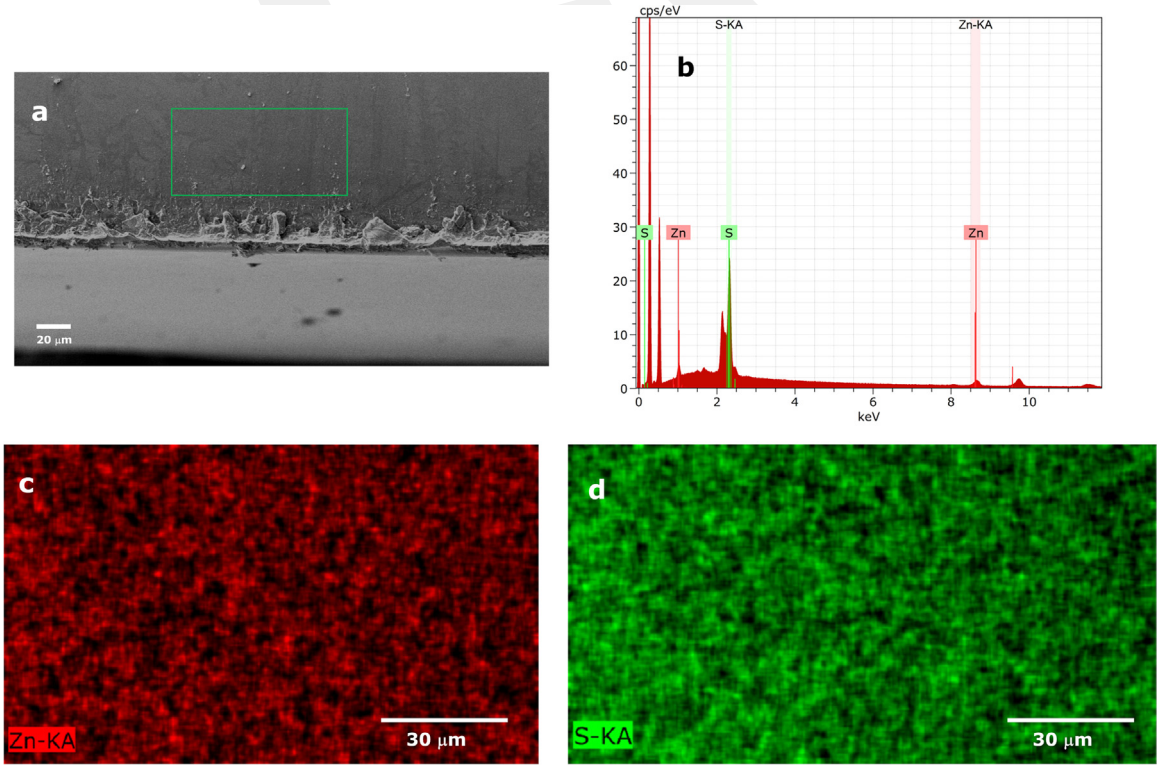

Fig. 9. EDX element mapping for Zn and from the cross section of the membrane with PVA:PAMPS:ZIF-8 (55:40:5) composition, (magnification of 2500 ×).

Table 1
Physicochemical properties of composite membranes.

PVA:PAMPS:ZIF-8 Ratio (wt%)	IEC (meq/g)	Water-Uptake (g/g)	Proton Conductivity (S/cm)	Activation Energy (kJ/mol)
85:10:05	**0.34**	**2.13**	**0.001**	**10.81**
75:20:05	**0.54**	**2.43**	**0.005**	**11.4**
65:30:05	**1.12**	**3.01**	**0.084**	**12.46**
55:40:05	**1.52**	**3.28**	**0.134**	**15.23**
60:40:00	**1.54**	**3.05**	**0.104**	**12.26**

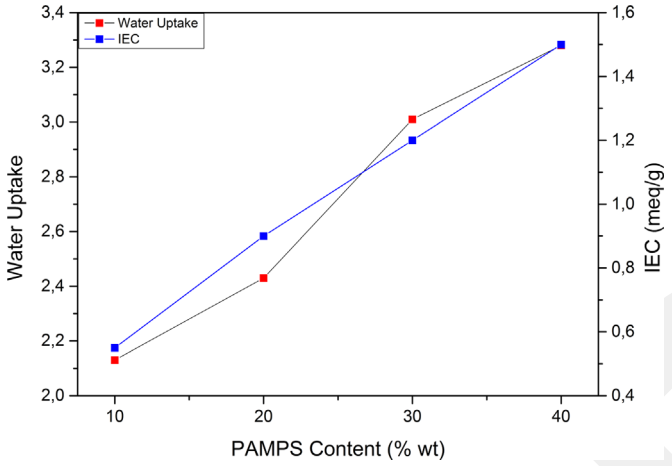

Fig. 10. Water uptake and IEC values of the membrane as a function of PAMPS content (wt%).

significantly. Generally, the proton conductivity increases with increasing IEC due to high charge density inside the membrane [4,8,37]. The IEC values of the prepared membranes are presented in Table 1. According to the results of these experiments, IEC values increase with the increasing PAMPS content (i.e. SO_3^{-1}) in the membrane. The highest IEC value of 1.52 mmol/g is achieved with PVA:PAMPS:ZIF-8 (55:40:5). Note that the membrane in this composition has a higher IEC value compared to Nafion-117 in the literature [4].

Fig. 10 shows the WU and IEC values of the membranes as a function of PAMPS content. From this figure, it can be seen that both WU and IEC values increase with increasing PAMPS content in the membrane. As a result of chemical cross-linking of PVA, the hydrophilic hydroxyl groups (–OH) in the PVA react with aldehyde groups (–CHO) in the GA. Therefore, the WU character of the membranes strongly depends on the hydrophilic sulfonic acid groups in PAMPS [8]. Additionally, sulfonic acid groups are the only ion exchangeable groups in the membrane, so the change in IEC values are directly linked to PAMPS content in the membrane. Both WU and IEC values are broadly consistent with similar studies in the literature, and they are considerably higher than those of Nafion in the literature [4,33,40].

3.7. *Proton conductivity*

Fig. 11 presents the Arrhenius plot of the proton conductivity for fully hydrated composite membranes. It shows that there is linear temperature dependence between 20 and 80 °C. Regardless of the compositions of the membranes, proton conductivities increase with temperature. As expected, the proton conductivity of the membranes increase with increasing the PAMPS content as well. For instance, the whereas conductivity of PVA:PAMPS:ZIF-8 (85:10:5) reached 0.001 S cm^{-1} at 80 °C, the conductivity of PVA:

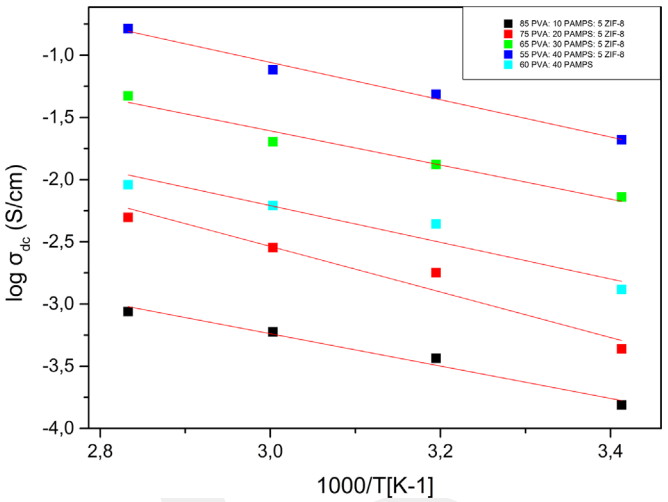

Fig. 11. Arrhenius plot for the proton conductivity of composite membranes.

PAMPS:ZIF-8 (55:40:5) reached 0.134 S cm^{-1} at 80 °C, which is 13 times higher than that of PVA:PAMPS:ZIF-8 (85:10:5). (Table 1) For comparison purposes, the proton conductivity values for fully hydrated Nafion -117 are between 0.09-0.1 S cm^{-1} in the literature [42]. On the other hand, in comparison to PVA:PAMPS (60:40), the membrane with PVA/PAMPS/ZIF-8 (55:40:5) has considerably higher proton conductivities. It may be concluded from these findings that ZIF-8 nanoparticles in the membrane contribute to the migration of protons. In that case, the hydrogen atoms on the outer surfaces of ZIF-8 nanoparticles contributed to the proton conduction pathway by making hydrogen bonding network with the polymer electrolyte. Additionally, the defect sites inside the ZIF-8 structure also facilitates the proton transfer by providing hydrogen bonding [25,43].

The activation energies, E_a, are derived from the Arrhenius plot of the composite membranes. The change in proton conductivity with temperature is given by Arrhenius equation:

$$\sigma = \sigma_0 \exp\left(-\frac{E_a}{kT}\right) \quad (2)$$

where k is the Boltzmann constant, E_a is the activation energy of proton conduction and T is temperature in terms of Kelvin. The slope of $\log \sigma$ vs $1000/T$ gives the activation energy of proton conduction. The obtained activation energies for the composite membranes are in between 10.81 and 15.23 kj mol^{-1}. These results are similar to the activation energy of Nafion-117 (12 kj mol^{-1}) [4]. According to these results, the proton migration across the membrane can attribute to three mechanisms. In the first mechanism, proton migration from one site to another is controlled by the formation and breaking of hydrogen bonds between a hydroxyl groups or water molecules (Grotthuss mechanism). In the composite membrane, the number of sulfonic acid groups may assist the Grotthuss mechanism. In the second vehicle-type mechanism, a proton combines with solvent molecules in the medium, producing a complex, which then diffuses. For instance, a proton combined with water molecule in the medium can migrate by hydronium ion (H_3O^+) through the channels of PVA polymeric domains [2,4,8,9,36,44]. In the third mechanism, protons are transferred inside the membrane along the hydrogen bonding path by generated ZIF-8 nanoparticles [25,43,45].

4. Conclusion

This study reports the preparation of a series of PVA:PAMPS:ZIF-8 proton conducting ternary composite membranes. The

findings of our research are quite convincing, and thus the following conclusions can be drawn: SEM and EDX micrograph confirm that all materials are uniformly distributed in the membrane. FT-IR spectra confirm the achievement of chemical crosslinking of PVA by GA and also indicate the existence of intermolecular interaction between the constituents. Thermal degradation result indicates that the composite membrane can be utilized up to 200 °C. Water uptake (WU) and ion exchange capacity (IEC) tests showed that both values directly link to the PAMPS content in the membrane and reached values are higher than those of Nafion for the same conditions in the literature. Among the membranes, the fully hydrated membrane with PVA:PAMPS:ZIF-8 (55:40:5) composition shows the best proton conductivity of 0.134 S cm^{-1}at 80 °C, which is comparable to commercial membrane, Nafion-117. In addition, this study shows the enhanced effects of ZIF-8 nanoparticles on proton conductivity. To the best our knowledge, this study represents one of the first example of a MOF-containing membrane with truly high proton conductivities and favorable properties. We believe that our findings may open new perspectives for the development of next-generation PEMs based on MOF structures.

Acknowledgements

This work was supported by The Scientific and Technological Research Council of Turkey TUBITAK under the contract No. 214M397 and partially granted by AGU-BAP under the contract No. FOA-2015-6.

References

[1] Y. Wang, et al., A review of polymer electrolyte membrane fuel cells: Technology, applications, and needs on fundamental research, Appl. Energy 88 (4) (2011) 981–1007.
[2] T. Hamaya, et al., Novel proton-conducting polymer electrolyte membranes based on PVA/PAMPS/PEG400 blend, J. Power Sources 156 (2) (2006) 311–314.
[3] J.L. Qiao, T. Hamaya, T. Okada, New highly proton conductive polymer membranes poly(vinyl alcohol)-2-acrylamido-2-methyl-1-propanesulfonic acid (PVA-PAMPS), J. Mater. Chem. 15 (41) (2005) 4414–4423.
[4] J.L. Qiao, T. Hamaya, T. Okada, Chemically modified poly(vinyl alcohol)-poly(2-acrylamido-2-methyl-1-propanesulfonic acid) as a novel proton-conducting fuel cell membrane, Chem. Mater. 17 (9) (2005) 2413–2421.
[5] U. Sen, et al., Enhancement of anhydrous proton conductivity of poly(vinylphosphonic acid)-Poly(2,5-benzimidazole) membranes via in situ polymerization, Macromol. Chem. Phys. 216 (1) (2015) 106–112.
[6] U. Sen, et al., Anhydrous proton conducting membranes for PEM fuel cells based on Nafion/Azole composites, Int. J. Hydrog. Energy 33 (11) (2008) 2808–2815.
[7] M. Higa, et al., Poly(vinyl alcohol)-based polymer electrolyte membranes for direct methanol fuel cells, Electrochim. Acta 55 (4) (2010) 1445–1449.
[8] J.L. Qiao, T. Hamaya, T. Okada, New highly proton-conducting membrane poly (vinylpyrrolidone)(PVP) modified poly(vinyl alcohol)/2-acrylamido-2-methyl-1-propanesulfonic acid (PVA-PAMPS) for low temperature direct methanol fuel cells (DMFCs), Polymer 46 (24) (2005) 10809–10816.
[9] C.P. Liu, et al., Novel proton exchange membrane based on crosslinked poly (vinyl alcohol) for direct methanol fuel cells, J. Power Sources 249 (2014) 285–298.
[10] W.L. Xu, et al., New proton exchange membranes based on poly (vinyl alcohol) for DMFCs, Solid State Ion. 171 (1–2) (2004) 121–127.
[11] M.S. Kang, et al., A highly charged proton exchange membranes prepared by using water soluble polymer blends for fuel cells, J. membr. Sci. 247 (1–2) (2005) 127–135.
[12] B. Smitha, S. Sridhar, A.A. Khan, Synthesis and characterization of poly(vinyl alcoho)-based membranes for direct methanol fuel cell, J. Appl. Polym. Sci. 95 (5) (2005) 1154–1163.
[13] B. Smitha, et al., Synthesis, characterization and application of crosslinked poly vinyl alcohol membranes for pervaporation and fuel cells, J. Polym. Mater. 22 (4) (2005) 433–444.
[14] L.E. Karlsson, B. Wesslen, P. Jannasch, Water absorption and proton conductivity of sulfonated acrylamide copolymers, Electrochim Acta 47 (20) (2002) 3269–3275.
[15] U. Sen, et al., Proton conducting polymer blends from poly(2,5-Benzimidazole) and poly(2-Acrylamido-2-methyl-1-propanesulfonic acid), J. Appl. Polym. Sci. 120 (2) (2011) 1193–1198.
[16] L.E. Karlsson, P. Jannasch, B. Wesslen, Preparation and solution properties of amphiphilic sulfonated acrylamide copolymers, Macromol. Chem. Phys. 203 (4) (2002) 686–694.
[17] D.J. Tranchemontagne, J.R. Hunt, O.M. Yaghi, Room temperature synthesis of metal-organic frameworks: MOF-5, MOF-74, MOF-177, MOF-199, and IRMOF-0, Tetrahedron 64 (36) (2008) 8553–8557.
[18] N. Stock, S. Biswas, Synthesis of metal-organic frameworks (MOFs): routes to various mof topologies, morphologies, and composites, Chem. Rev. 112 (2) (2012) 933–969.
[19] H. Furukawa, et al., The chemistry and applications of metal-organic frameworks, Science 341 (6149) (2013) 974.
[20] Y.X. Ye, et al., High anhydrous proton conductivity of lmidazole-loaded mesoporous polyimides over a wide range from subzero to moderate temperature, J. Am. Chem. Soc. 137 (2) (2015) 913–918.
[21] M. Sadakiyo, T. Yamada, H. Kitagawa, Rational designs for highly proton-conductive metal-organic frameworks, J. Am. Chem. Soc. 131 (29) (2009) 9906.
[22] J.M. Taylor, et al., Facile proton conduction via ordered water molecules in a phosphonate metal-organic framework, J. Am. Chem. Soc. 132 (40) (2010) 14055–14057.
[23] N.C. Jeong, et al., Coordination-chemistry control of proton conductivity in the iconic metal-organic framework material HKUST-1, J. Am. Chem. Soc. 134 (1) (2012) 51–54.
[24] S.S. Nagarkar, et al., Two-in-One: inherent anhydrous and water-assisted high proton conduction in a 3d metal-organic framework, Angew. Chem. Int. ed. 53 (10) (2014) 2638–2642.
[25] P. Barbosa, et al., Protonic conductivity of nanocrystalline zeolitic imidazolate framework 8, Electrochim. Acta 153 (2015) 19–27.
[26] K.S. Park, et al., Exceptional chemical and thermal stability of zeolitic imidazolate frameworks, Proc. Natl. Acad. Sci. USA 103 (27) (2006) 10186–10191.
[27] B.L. Chen, et al., Zeolitic imidazolate framework materials: recent progress in synthesis and applications, J. Mater. Chem. A 2 (40) (2014) 16811–16831.
[28] J.F. Yao, H.T. Wang, Zeolitic imidazolate framework composite membranes and thin films: synthesis and applications, Chem. Soc. Rev. 43 (13) (2014) 4470–4493.
[29] J.A. Gee, et al., Adsorption and diffusion of small alcohols in zeolitic imidazolate frameworks ZIF-8 and ZIF-90, J. Phys. Chem. C 117 (6) (2013) 3169–3176.
[30] K. Zhang, et al., Exploring the framework hydrophobicity and flexibility of ZIF-8: from biofuel recovery to hydrocarbon separations, J. Phys. Chem. Lett. 4 (21) (2013) 3618–3622.
[31] K. Zhang, et al., Investigating the intrinsic ethanol/water separation capability of ZIF-8: an adsorption and diffusion study, J. Phys. Chem. C 117 (14) (2013) 7214–7225.
[32] J. Cravillon, et al., Rapid room-temperature synthesis and characterization of nanocrystals of a prototypical zeolitic imidazolate framework, Chem. Mater. 21 (8) (2009) 1410–1412.
[33] C.E. Tsai, C.W. Lin, B.J. Hwang, A novel crosslinking strategy for preparing poly (vinyl alcohol)-based proton-conducting membranes with high sulfonation, J. Power Sources 195 (8) (2010) 2166–2173.
[34] H. Gao, K. Lian, Advanced proton conducting membrane for ultra-high rate solid flexible electrochemical capacitors, J. Mater. Chem. 22 (39) (2012) 21272–21278.
[35] M. Amirilargani, B. Sadatnia, Poly(vinyl alcohol)/zeolitic imidazolate frameworks (ZIF-8) mixed matrix membranes for pervaporation dehydration of isopropanol, J. Membr. Sci. 469 (2014) 1–10.
[36] X.X. Chen, G.B. Guo, Studies on preparation and properties of SiO2/PVA-PAMPS composite Membrane, Renew. Sustain. Energy II 512–515 (2012) 2007–2010 1-4.
[37] C.A. Dai, et al., Polymer actuator based on PVA/PAMPS ionic membrane: optimization of ionic transport properties, Sens. Actuators A-Phys. 155 (1) (2009) 152–162.
[38] C.C. Yang, S.J. Lue, J.Y. Shih, A novel organic/inorganic polymer membrane based on poly(vinyl alcohol)/poly(2-acrylamido-2-methyl-1-propanesulfonic acid/3-glycidyloxypropyl trimethoxysilane polymer electrolyte membrane for direct methanol fuel cells, J. Power Sources 196 (10) (2011) 4458–4467.
[39] Immunosuppressive, Therapy and inflammatory bowel disease after transplantation, Liver Transplant. 14 (12) (2008) 1812–1813.
[40] C.W. Lin, Y.F. Huang, A.M. Kannan, Cross-linked poly(vinyl alcohol) and poly (styrene sulfonic acid-co-maleic anhydride)-based semi-interpenetrating network as proton-conducting membranes for direct methanol fuel cells, J. Power Sources 171 (2) (2007) 340–347.
[41] J. Fu, et al., Alkali doped poly(vinyl alcohol) (PVA) for anion-exchange membrane fuel cells-Ionic conductivity, chemical stability and FT-IR characterizations, Alkaline Electrochem. Power Sources 25 (13) (2010) 15–23.
[42] S. Ochi, et al., Investigation of proton diffusion in Nafion (R) 117 membrane by electrical conductivity and NMR, Solid State Ion. 180 (6–8) (2009) 580–584.
[43] X.Q. Liang, et al., From metal-organic framework (MOF) to MOF-polymer composite membrane: enhancement of low-humidity proton conductivity, Chem. Sci. 4 (3) (2013) 983–992.
[44] C.A. Dai, et al., A membrane actuator based on an ionic polymer network and carbon nanotubes: the synergy of ionic transport and mechanical properties, Smart Mater. Struct. 18 (2009) 8.
[45] B. Wu, et al., Oriented MOF-polymer composite nanofiber membranes for high proton conductivity at high temperature and anhydrous condition, Sci. Rep. 4 (2014) 1–7.